

Supporting information for molecular dynamics simulation of adsorption and separation of xylene isomers by Cu-HKUST-1

*Guo-Jian Ji ^{*a, b}, Ting Xiang ^a, Xiao-Qing Zhou ^a, Le Chen ^b, Zhi-Hui Zhang ^b,*

Bei-Bei Lu ^a and Xing-Jian Zhou ^a

*a. Jiangsu Key Laboratory of Green Process Equipment, School of Petroleum and Gas
Engineering, School of Energy, Changzhou University, Changzhou, 213164, P. R.*

China. Address here.

*b. Jiangsu Key Laboratory of Advanced Catalytic Materials and Technology, Advanced
Catalysis and Green Manufacturing Collaborative Innovation Center, Changzhou
University, Changzhou 213164, P. R. China.*

** Corresponding Author: Phone:86-15806128724. E-mail: jgj@cczu.edu.cn*

S1 Characterization of xylenes

Table S1 Physical properties of xylene isomers.¹⁻²

	PX	MX	OX
Kinetic diameter (Å)	5.9	6.8	7.1
Molecular length (Å)	9.2	8.6	8.0
Molecular width (Å)	6.7	7.4	7.5
Boiling point (K)	411.4	412.1	417.4
Freezing point (K)	286.4	222.5	248.0
Dipolemoment (D)	0	0.24	0.62 (gas)
Polarizability (Å ³)	14.2	14.2	14.9
Density at 25°C (g.cm ⁻³)	0.858	0.861	0.876

Description: The kinetic diameter is the actual particle size replaced by the equivalent diameter with the same aerodynamic properties.

S2 Force field parameters

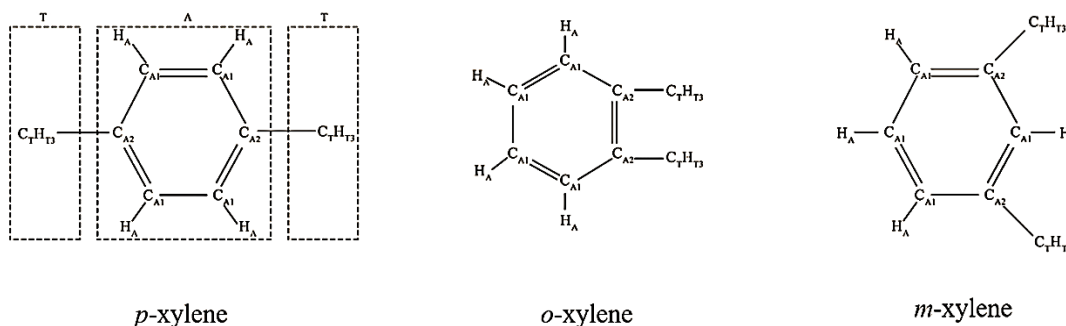


Fig. S1 Isomeric structure of xylene.

Table S2 Partial charge and potential parameters for non-bonded interactions.³

Atomic Type	Atomic mass (amu)	Partial charge (e ⁻)
CA ₁	12.011	-0.205
CA ₂	12.011	0.180
C _T	12.011	-0.222
H _A	1.008	0.130
H _T	1.008	0.064

Lennard-Jones 12-6 parameters	Pair coefficient	
	ϵ_{ij} (K _{cal} /mol)	σ_{ij} (Å)

C _A -C _A	0.0859	3.40
C _A -C _T	0.0970	3.40
C _A -H _A	0.0359	3.00
C _A -H _T	0.0367	3.02
C _T -C _T	0.1093	3.40
C _T -H _A	0.0405	3.00
C _T -H _T	0.0422	3.02
H _A -H _A	0.0150	2.60
H _A -H _T	0.0153	2.62
H _T -H _T	0.0157	2.65

Table S3 Potential parameters for bonding interactions.³

Bond	Bond Parameters		
	k_r (Kcal/mol. Å ²)	r^0 (Å)	
C _A -C _A	938.00	1.409	
C _A -H _A	734.00	1.080	
C _A -C _T	634.00	1.522	
C _T -H _T	680.00	1.090	
Angle	Angle Parameters		
	k^θ (Kcal/mol.rad ²)	θ^0 (deg)	
C _A -C _A -C _A	126.00	120.00	
C _A -C _A -H _A	70.00	120.00	
C _A -C _A -C _T	140.00	120.00	
C _A -C _T -H _T	100.00	109.50	
H _T -C _T -H _T	70.00	109.50	
Dihedral angle	Dihedral Angle Parameters		
	k (Kcal/mol)	n	δ (deg)
X-C _A -C _A -X	14.50	2	180.00
X-C _A -C _T -X	0.00	2	0.00

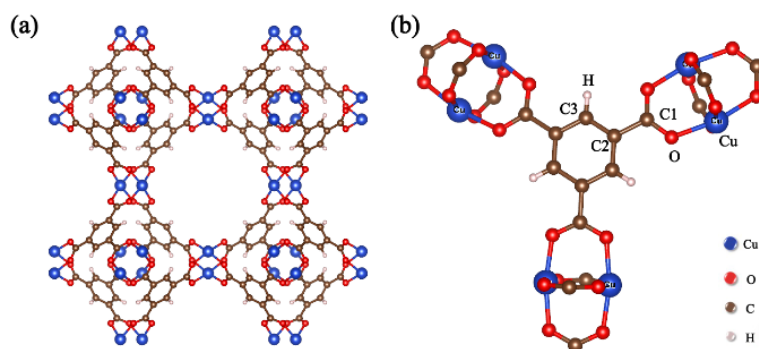


Fig. S2 Cu-HKUST-1.

Table S4 Partial charge and LJ parameter of Cu-HKUST-1.⁴

Atomic type	Atomic partial charge (e ⁻)	ϵ (kcal/mol)	σ (Å)
Cu	1.026	0.180	3.1136
H	0.123	0.044	2.5711
O	-0.671	0.060	3.1181
C1	0.875	0.105	3.4308
C2	-0.197	0.105	3.4308
C3	0.028	0.105	3.4308

S3 Simulation method

GCMC calculation: The gas adsorption properties of MOF are usually calculated by using Grand Canonical Monte Carlo (GCMC) simulations. To create Settings for gas molecules within the pores of the MOF, a series of random moves such as insertion, deletion, translation, rotation, and regeneration was used in the GCMC simulation, with different configurations of Boltzmann probabilities used as control parameters to accept or reject these moves. In Monte Carlo simulations, the number of simulation cycles used for the initialization and equilibration steps should be sufficient for the system to reach equilibrium such that the average number of gas adsorbed gas molecules (N) is the main result of the GCMC simulation.⁵

DFT calculation: Based on density functional theory (DFT), we used Vienna AB-Initio Simulation Package (VASP) version 6.1 to calculate the average effective charge of atoms.⁶ Considering the remote electrostatic interaction between Cu-HKUST-1 atoms and gas molecules, Because of the strong van der Waals force interaction between the hydrogen atom and other atoms, DFT-D3 correction is used.⁷ The Generalized Gradient Approximation (GGA) function and the Perdew Burke Ernzerhof (GGA-PBE) exchange-correlation method were used for all DFT calculations 36. The Projected Enhanced Wave (PAW) method solved the Kohn-Sham equation. In the Self-Consistent Field (SCF) iteration, the force and energy convergence thresholds were set to 0.02 eV/Å and 10⁻⁵ eV, respectively. The average effective charge (ΔQ) analysis was calculated from Eq. 1.

$$\Delta Q = Z_{val} - Q^{Bader} \quad (1)$$

Z_{val} and Q^{Bader} are the numbers of valence electrons and Bader charge per atom, respectively. Thus, positive or negative values of ΔQ indicate the number of Bard charges lost or gained within a single atom.

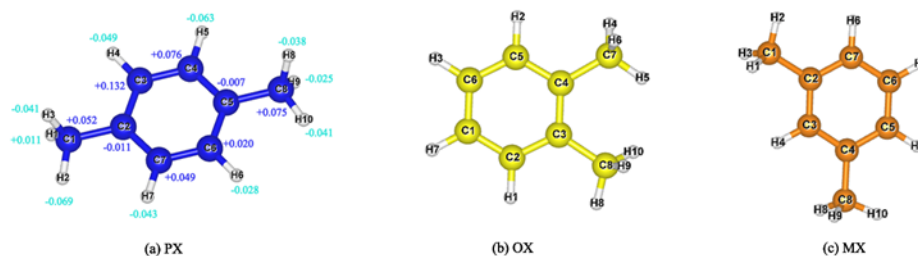


Fig. S3 The atomic type of xylenes in DFT.

Table S5 Charge from DFT.

Atomic sequence	Charge from DFT (e ⁻)		
	PX	MX	OX
H1	0.011	0.016	3.126
H2	-0.069	-0.063	3.054
H3	-0.041	-0.056	2.967
H4	-0.049	-0.070	3.046
H5	-0.063	-0.054	3.031
H6	-0.028	-0.035	3.041
H7	-0.043	-0.044	3.031
H8	-0.038	-0.050	3.037
H9	-0.025	-0.009	-0.029
H10	-0.041	-0.044	-0.038
C1	0.052	0.055	-3.064
C2	-0.011	-0.009	-2.998
C3	0.132	0.169	-3.028
C4	0.076	-0.071	-3.039
C5	-0.007	0.077	-3.057
C6	0.020	0.048	-3.011
C7	0.049	0.061	-3.038
C8	0.075	0.079	-3.031

S4 Experimental methods

Fourier Transform (FT) infrared data were recorded on an Avatar-370 (Nicolet) spectrometer by sample transfer deposited on KBr particles. Powder X-ray Diffraction (PXRD) (Fig. S4) patterns of the synthesized and recovered samples were obtained using a Rigaku D/Max 2500 PC X-ray diffractometer using Cu K α (1.5406 Å) radiation at 10°·min⁻¹. Thermogravimetric analysis (TGA) experiments were performed on a TG/DTA 6300 thermal analyzer from room temperature to 800 °C at a heating rate of 10 °C·min⁻¹ in a nitrogen atmosphere. Field-emission SEM images of the samples were taken with a Zeiss Supra 55 microscope at 30 kV. TEM images were taken on a JEOL JEM2 100 transmission electron microscope at an accelerating voltage of 200 kV. The composition of the samples was analyzed by ICP (Inductively Coupled Plasma) analysis (Varian Vista-AX). N₂ adsorption isotherms were obtained using a Micromeritics ASAP 2460 instrument. Samples were degassed at 150 °C for an eighth before measurement. X-ray photoelectron spectroscopy (XPS) was used to analyze physical electron PHI-550 light equipped with an Al K α X-ray source (HV = 1486.6 eV). Per the spectrometer, the operating voltage is 10 kV and 35 mA.

A liquid equivalent binary breakthrough experiment studied the dynamic adsorption separation of xylene isomers. To test reproducibility, three parallel dynamic experiments were performed for each condition. The experimental procedures and instruments are the same as those in the literature.⁸ Stainless steel column (10 cm long, 1.0 cm inner diameter), filled with the adsorbent (1.0⁻² g) and quartz sand at the bottom, placed in an oven to adjust the adsorption temperature. The operation was performed by sequential introduction of xylene allosomes of known components (OX: PX = 1:1, OX: MX = 1:1, OX: MX = 1:1). MX: PX = 1:1, isooctane was used as the solvent in the imported mixture (60%), and the total flow rate was adjusted to 0.5 ml·min⁻¹ at standard atmospheric pressure. When saturation was reached, the composition of each sample was analyzed by Flame Ionization Detection (FID) using a Shimadzu GC2010 chromatographic system.

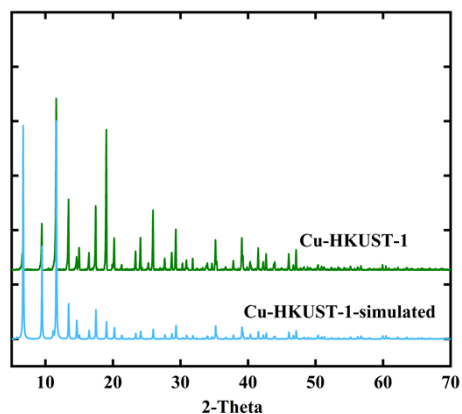


Fig. S4 Powder X-ray diffraction (PXRD) patterns of Cu-HKUST-1 microcrystals.

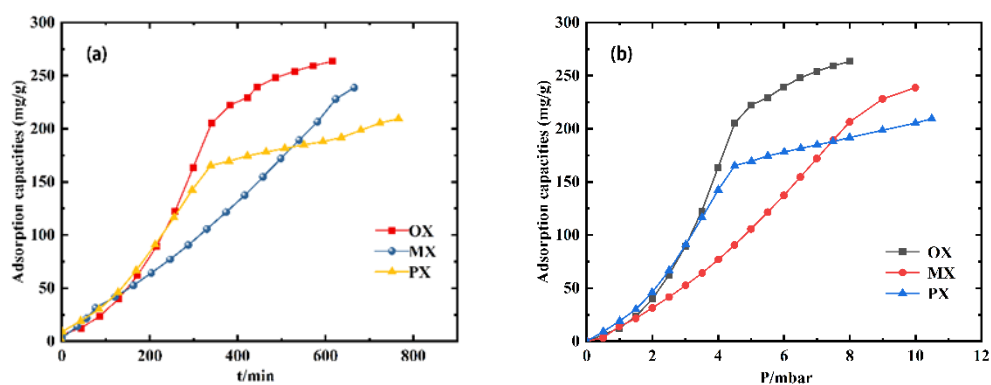


Fig. S5 Single component vapor-phase adsorption rate curves for OX, MX and PX on Cu-HKUST-1.

S5 Characterization details of Cu-HKUST-1

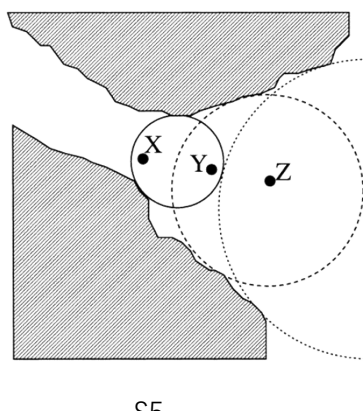


Fig. S6. Two-dimensional geometric derivation of aperture distribution. Minimum (solid) circles can only cover point "x", point "y" can be covered by minimum and medium (dotted) circles, and all three loops can cover point "z". We obtain a cumulative pore volume curve by determining the maximum cover circle at each point in the pore volume. (This figure is from reference ⁹ as the theoretical basis of PSD analysis.)

Table S6 Cu-HKUST-1 structure parameters.

Parameter Type	Structure Parameters
Density (g/cm ³) ¹⁰	0.88
Porosity ϕ (Å)	6.5
S_{BET} (m ² /g)	1718
V_{free} (cm ³ /g)	0.68
Larger Cavity Diameter LCD (Å)	12
Pore Limit Diameter PLD (Å)	4.6

Zeo++ was used to calculate the surface area of Cu-HKUST-1 cell structure accessible to the Aspherical probe (N₂ probe was used in this simulation, 3.681Å). Specifically, the surface area accessible to the center of the investigation. The calculation is carried out in two steps. First, the accessibility of the channel is determined, and then the Monte Carlo sampling method is used to score the area. One of the nitrogen probe molecules rolls along the surface of the frame, and the surface area of the unit cell Cu-HKUST-1 is 3518.63 Å².

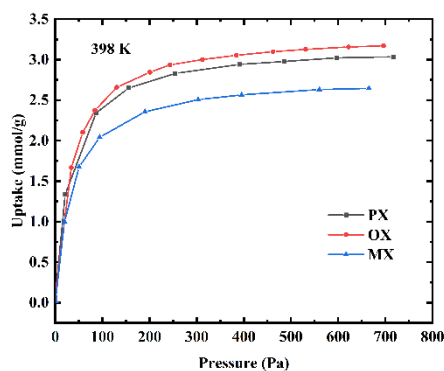


Fig. S7 The single component adsorption isotherm obtained in the 398K breakthrough experiment.

S6 Comparison of fitted models

S7 Comparison of fitted models

Table S7 Xylene isomer adsorption model.

Type	Model	Equation	Note
1	Langmuir	$q = kbp / (k + bp)$	q is the absolute adsorption amount; k is the saturation adsorption amount; b is the adsorption constant; p is the adsorption pressure.
2	Freundlich	$q = Kp^{1/n}$	K is an empirical constant, q can be considered as the amount of adsorption per unit pressure; n is a temperature-dependent parameter, and p reflects the magnitude of the adsorption intensity.

Table S8 Langmuir and Freundlich fitting constants and correlation coefficients of absolute adsorption capacity curves.

T (K)	Type	Langmuir			Freundlich		
		$k(\text{mmol/g})$	b/Pa^{-1}	r^2	$K(\text{mg/g})$	n	r^2
348	PX	1.730	0.110	0.965	0.644	6.564	0.772
	OX	1.743	0.105	0.970	0.644	6.530	0.776
	MX	1.221	0.163	0.962	0.576	8.521	0.585
373	PX	1.321	0.026	0.975	0.316	4.185	0.819
	OX	1.321	0.023	0.979	0.294	3.991	0.836
	MX	1.284	0.021	0.957	0.285	4.589	0.789
398	PX	2.057	0.004	0.960	0.033	1.815	0.915
	OX	2.061	0.004	0.961	0.030	1.782	0.917
	MX	2.056	0.004	0.962	0.033	1.907	0.910

Note: Using the correlation coefficient r^2 as a criterion, the fitting results showed that the Langmuir equation fitted the absolute adsorption curves better than the Freundlich equation above the critical temperature.

S8 Comparison of adsorption density

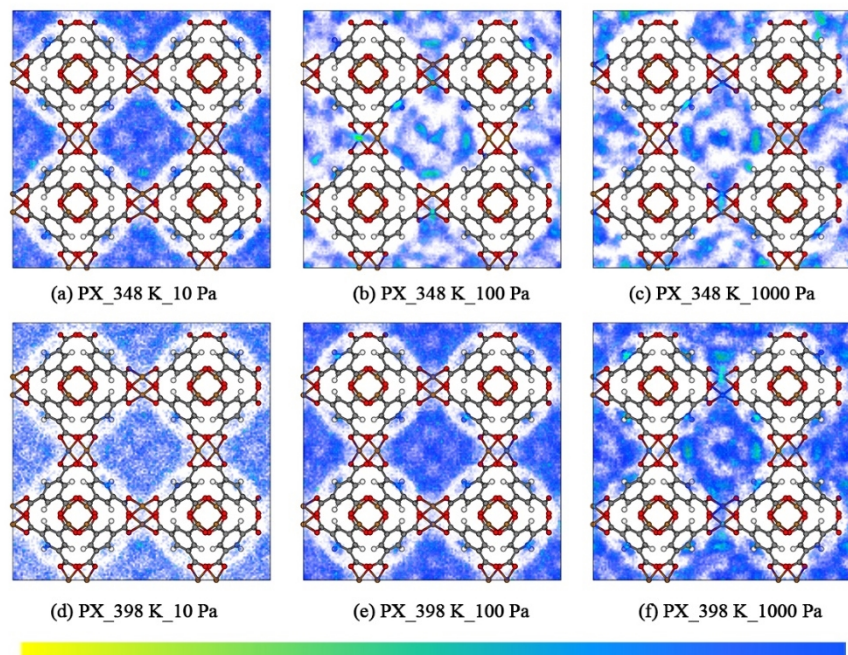


Fig. S8 Adsorption density of PX at 348 K and 398 K. (10 Pa, 100 Pa, and 1000 Pa).

REFERENCES

- 1 T. G. Grissom, C. H. Sharp, P. M. Usov, D. Troya, A. J. Morris and J. R. Morris, *J. Phys. Chem. C.*, 2018, **122**, 16060–16069.
- 2 D. I. Kolokolov, H. Jobic, A. G. Stepanov, J. Ollivier, S. Rives, G. Maurin, T. Devic, C. Serre and G. Férey, *J. Phys. Chem. C.*, 2012, **116**, 15093–15098.
- 3 A. K. Rappe, C. J. Casewit, K. S. Colwell, W. A. I. Goddard and W. M. J. Skiff, *J. Am. Chem. Soc.*, 1992, **114**, 10024–10035.
- 4 A. M. Thomas and S. S. David, *J. Chem. Theory Comput.*, 2010, **6**, 2455–2468
- 5 J. P. Nan, X. L. Dong, W. J. Wang, W. Q. Jin and N. P. Xu, *Langmuir*, 2011, **27**, 4309–4312.
- 6 X. J. Zhou, Y. L. Sun, B. Z. Zhu, J. Y. Chen, J. C. Xu, H. L. Yu and M. G. Xu, *Fuel*, 2022, **318**, 123470.
- 7 R. Babarao, J. Jiang, S. I. Sandler, *Langmuir*, 2009, **25**, 5239.
- 8 T. X. Yan, X. J. Li, L. Chen, Z. H. Zhang, Q. Chen and M. Y. He, *J. Solid State Chem.*, 2022, **307**, 122819.
- 9 L. D. Gelb, and K. E. Gubbins, *Langmuir*, 1999, **15**, 305–308.
- 10 D. Peralta, K. Barthelet, J. Pérez-Pellitero, C. Chizallet, G. Chaplais, A. Simon-Masseron and G. D. Pirngruber, *J. Phys. Chem. C.*, 2012, **116**, 21844–21855.